Neural Controller Based Full Vehicle Nonlinear Active Suspension Systems with Hydraulic Actuators

Ammar A. Aldair and Weiji J. Wang
School of Engineering and Design, University of Sussex
Brighton, BN1 9QT, UK
aa386@sussex.ac.uk, w.j.wang@sussex.ac.uk

Abstract

This paper is concerned with full vehicle nonlinear active suspension systems, in which each suspension unit consists of three components: a nonlinear spring, a nonlinear damper and a nonlinear hydraulic actuator. An artificial intelligence Neural Control technique has been presented in this paper to design a robust controller for full vehicle nonlinear active suspension systems. The advantage of this controller is that it can handle the nonlinearities faster than other conventional controllers. Neural controller are devised to adjust the hydraulic actuators forces to minimize the vertical displacement at each suspension point when travelling on rough roads and to reduce the inclination of the vehicle during sudden manoeuvres such as sharp bending and braking. The robustness of the proposed controller is being assessed by comparing with Fractional Order PI^iD^d (FOPID) controller. To validate the robustness of the proposed approach, the cases with six types of disturbances will be investigated. The results show that intelligent neural controller have improved dynamic response measured by a decreased cost function.

Keywords: *Full vehicle, Nonlinear Active Suspension System with Hydraulic Actuators, Neural Controller.*

1. Introduction

In recent years, several models and controllers have been developed in attempts to improve the ride and handling qualities for modern vehicles. In publications [1-9], quarter or half vehicle linear model was used to design the control system, while it could only indicate the vehicle body vertical movement or/and the pitching movement, not the rolling movement of vehicle.

Therefore, importantly, a full vehicle model must be introduced to take into account the heave, pitching and rolling movements. Gaspar et al. in Reference [10] have used a robust controller for a full vehicle linear active suspension system using the mixed parameter synthesis. A sliding mode technique is designed for a linear full vehicle active suspension system [11]. A method is developed for the purpose of sensor fault diagnosis and accommodation. In Reference [12], the authors presented the development of an integrated control system of active front steering and normal force control using fuzzy reasoning to enhance the full vehicle model handling performance.

Due to the fact that strong nonlinearity inherently exists in the damper and spring components [13-15], inevitably the nonlinear effect must be taken into account in designing the controller for practical active suspension systems. This paper will be developed a model for full vehicle nonlinear active suspension systems with hydraulic actuators to take into

account the three motions of the vehicle: vertical movement at centre of gravity, pitching movement and rolling movement.

An intelligent controller can be used to design a control system for a full vehicle nonlinear active suspension system such as Neural Controller (NC). Neural Networks (NNs) are capable of handling complex and nonlinear problems, process information rapidly and can reduce the engineering effort required in controller model development. Artificial neural networks are made up of a simplified individual models of the biological neuron that are connected together to form a network. It consists of a pool of simple processing units which communicate by sending signals to each other over a large number of weighted connections. Capability of learning information by example; ability to generalize to new input and robustness to noisy data are the important properties of neural networks. From these properties, neural networks are able to solve complex problems that are currently intractable.

The artificial neural network is an intelligent device wildly used to design robust controllers for nonlinear processes in engineering problems. In many publications, neural networks are used to design controllers, such as the model reference adaptive control, model predictive control, nonlinear internal model control, adaptive inverse control system and neural adaptive feedback linearization [16, 17]. The control architectures in these papers depend on designing a neural network identifier and then this identifier is used as a path to propagate the error between the output of the process and output of the reference model to train and select the optimal values of the neural network control. Therefore, in those methods two neural networks were trained to track several control objectives.

One of the main advantages of using a neural network as a controller is that neural networks are universal function approximations which learn on the basis of examples and may be immediately applied in an adaptive control system because of their capacity to adapt in real time. There are many learning algorithms available to obtain the optimal values of the trainable parameters of neural network. The back-propagation algorithm (BPA) has been known as an algorithm with a very poor convergence rate. The Levenberg-Marquardt Algorithm (LMA) is an iterative technique that locates the minimum of a multivariate function that is expressed as the sum of squares of nonlinear real-valued functions [18, 19].

To improve the riding comfort and road handling, a neural network controller for full vehicle nonlinear active suspension systems with hydraulic actuators has been proposed by the authors. In this paper Fractional Order PIlDd (FOPID) will be designed for full vehicle nonlinear active suspension using the Evolutionary Algorithm (EA). The data obtained from the FOPID controller are used as reference to design the neural controller. The Levenberg-Marquardt training algorithm has been used to obtain the optimal values of the trainable parameters. The performance of the neural controller has been improved by adding the Scaling Gains. The scaling gains of the neural controller have been adjusted using Golden Section Search (GSS) method. The effectiveness and robustness of the proposed neural network controller and FOPID controller will be compared. Six types of the disturbances will be investigated to establish the robustness of the proposed controller. The results will show whether the proposed controller is more robust than the FOPID controller.

2. Mathematical Model of the Controlled System

The main purposes of active suspension controller are to increase both riding comfort and handling quality. The riding comfort can be measured by evaluating the acceleration and displacement of sprung mass. The handling quality can be achieved by controlling the rotational motions of the vehicle body such as rolling and pitch movements during cornering and braking. Figure 1 illustrates the full vehicle nonlinear active suspension systems with

hydraulic actuators. In this model the tyres are modeled as linear spring in parallel with linear viscous dampers. However, the suspension part is modeled as a nonlinear hydraulic actuator in parallel with a nonlinear damper and a nonlinear spring. The nonlinear frictional forces due to rubbing of piston seals with the cylinders wall inside the actuators are taken into account to calculate the real supply forces generated by the hydraulic actuator.

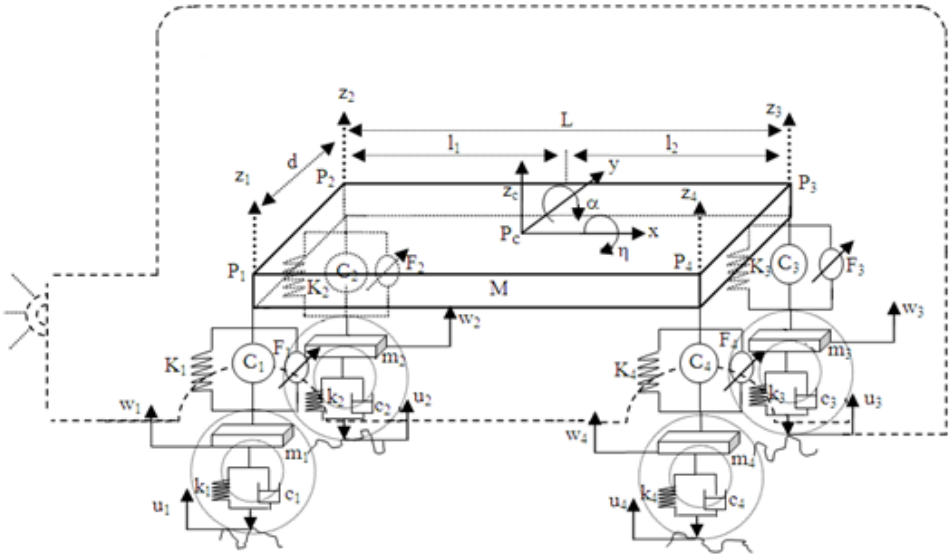

Figure 1 Full Vehicle Nonlinear Active Suspension System

The following equations of motion are derived for the full vehicle model using Newton laws of motion:

I. Vertical motion

$$M\ddot{z}_c = -\sum_{i=1}^{4} F_{Ki} - \sum_{i=1}^{4} F_{Ci} + \sum_{i=1}^{4} F_{Pi} \qquad (1)$$

where F_{Ki} and F_{Ci} are the nonlinear suspension spring force and nonlinear suspension damping force, respectively, which can be written as [20]

$$F_{Ki} = K_i(z_i - w_i) + \xi K_i(z_i - w_i)^3$$
$$F_{ci} = C_i(\dot{z}_i - \dot{w}_i) + \xi C_i(\dot{z}_i - \dot{w}_i)^2\, sgn(\dot{z}_i - \dot{w}_i)$$

The force generated by hydraulic actuator can be written as

$$F_{Pi} = F_{Ai} - F_{fi}$$

where F_{Ai} is the nonlinear hydraulic force provided by the i^{th} actuator and F_{fi} the nonlinear frictional force due to rubbing of piston seals with the cylinder wall inside the i^{th} actuator. The relation between the spool valve velocity, $\dot{x}_{vi}$, and the output force of this actuator, $F_{Ai} = A_p P_{Li}$, possess a nonlinear dynamic behaviour [21].

$$\dot{F}_{Ai} = A_p \alpha [C_d \omega x_{vi} \sqrt{\frac{P_{si} - sgn(x_{vi}) P_{Li}}{\rho}} - C_{tm} P_{Li} - A_p (\dot{z}_i - \dot{w}_i)] \quad (2)$$

The frictional force is modeled with a smooth approximation of Signum function:

$$F_{fi} = \begin{cases} \kappa \, sgn(\dot{z}_i - \dot{w}_i) \;\; if \;\; |\dot{z}_i - \dot{w}_i| > 0.01 \\ \kappa \, sin\left(\dfrac{\dot{z}_i - \dot{w}_i}{0.01} \dfrac{\pi}{2} \right) \;\; if \; |\dot{z}_i - \dot{w}_i| < 0.01 \end{cases} \quad (3)$$

II. Pitching motion

$$\begin{aligned} J_x \ddot{\alpha} = & (F_{K1} - F_{K2} - F_{K3} + F_{K4}) \frac{b}{2} + \\ & (F_{C1} - F_{C2} - F_{C3} + F_{C4}) \frac{b}{2} + \\ & (F_{P4} - F_{P1} + F_{P3} - F_{P2}) \frac{b}{2} + T_x \end{aligned} \quad (4)$$

where b is the distance between the front wheels (or rear wheels).

III. Rolling motion

$$\begin{aligned} J_y \ddot{\eta} = & (F_{K3} + F_{K4}) l_2 - (F_{K1} + F_{K2}) l_1 + \\ & (F_{C3} + F_{C4}) l_2 - (F_{C1} + F_{C2}) l_1 + \\ & (F_{P1} + F_{P2}) l_1 + (F_{P3} + F_{P4}) l_2 + T_y \end{aligned} \quad (5)$$

where l_1 is the distance between the centre of front wheel axle and centre of gravity of the vehicle. l_2 is the distance between the centre of gravity of the vehicle and the centre of rare wheel axle.

The motion of the i^{th} unsprung mass is governed by the following equation:

$$m_i \ddot{w}_i = -k_i (w_i - u_i) - c_i (\dot{w}_i - \dot{u}_i) + F_{Ki} + F_{Ci} - F_{Pi} \quad (6)$$

3. The structure of Neural Network:

Neural network architecture is quite simple to create and involves two or more neurons combined to form one or more layers. Figure 2 depicts the structure of multilayer neural network (or some time called multilayer perceptron network). In this figure, the neural network model has three layers: input layer, hidden layer and output layer. The input layer represents the input variables related to the problem. The output layer represents the desire output response of the system. The nodes in the hidden layer and output layer are the processing elements that allow the network to develop a behavioural representation of the problem space being addressed. Processing of the input information occurs at each of the hidden and output nodes within the network and is computationally relatively simple. Each node in the particular layer of the network is connected to all of the nodes in the previous layer. There is a weight value associated with each of the connection between nodes. The weighted inputs to a particular node are summed and the resultant value is passed through a

nonlinear activation function to determine the output value of the node. Therefore, each node has multiple inputs and single output.

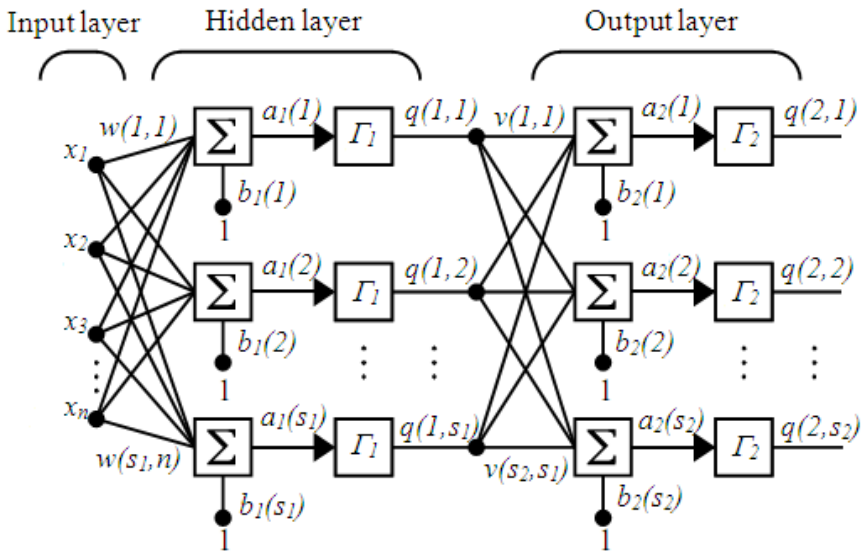

Figure 2 Multilayers Neural Network

The output of the k^{th} node in the hidden layer can be given as:

$$q(1,k) = \Gamma_1\left(\sum_{i=1}^{n} w(k,i)x_i + b_1(k)\right) \quad k = 1,2,\ldots,s_1 \tag{7}$$

where $q(1,k)$ is the output of the k^{th} node in the hidden layer, Γ_1 is the activation function of the hidden layer, $w(k,i)$ is the weight between i^{th} input and k^{th} node, x_i is the i^{th} input and $b_1(k)$ is the bias of the k^{th} node.

The output of the l^{th} node in the output layer can be given as

$$q(2,l) = \Gamma_2\left(\sum_{j=1}^{s_1} v(j,l)q(1,j) + b_2(l)\right) \quad l = 1,2,\ldots,s_2 \tag{8}$$

where $q(1,l)$ is the output of the l^{th} node in the output layer, Γ_2 is the activation function of the output layer, $v(j,l)$ is the weight between j^{th} node and l^{th} node, $q(1,j)$ is the j^{th} output of the hidden layer and $b_2(l)$ is the bias of the l^{th} node.

There are many training algorithms which can be used to determine the optimal values for the trainable parameters (weights and biases) between each of the nodes to minimise a Mean Squared Error (MSE) function

$$MSE = \frac{1}{2P}\sum_{i=1}^{P}\sum_{j=1}^{s_2}(q_i(2,j) - T_i(j))^2 \tag{9}$$

Where P is the number of data for each epoch, $q_i(2,j)$ is the output of j^{th} node in the output layer for i^{th} epoch and $T_i(j)$ is the j^{th} desire output for i^{th} epoch.

4. Levenberg-Marquardt Training Algorithm

The training phase of the neural networks required a set of examples of proper network behaviour i.e. network inputs and target output. The trainable parameters of neural network are adjusted during training phase to minimize the mean squared error (MSE) between the

neural network outputs and the target outputs. At the first iteration, the trainable parameters of the neural network are randomly initialized. The neural network processes each input vector and the output of the neural network is compared with the desired output (target output).

The Back-Propagation Algorithm has been a significant improvement in neural network researches [22-26]. The simplest implementation of backpropagation learning updates trainable parameters in the direction in which the performance function (mean squared error) decreases most rapidly (the negative of the gradient). The Backpropagation Algorithm has been known as an algorithm with a very poor converging rate for practical problems [27]. Many researches were carried out to accelerate the convergence of the algorithm. These researches focused on two different categories. The first category uses heuristic techniques, which were developed from an analysis of the performance of the backpropagation algorithm [28-30]. There are three different heuristic techniques: Momentum Technique, Variable Learning Rate Technique and Resilient Technique. In the second category of fast algorithms uses standard numerical optimization techniques. There are three main techniques of numerical optimization: Conjugate Gradient Technique [31], Quasi-Newton Technique [32] and Levenberg Marquardt Technique [33].

The Conjugate Gradient Technique produces generally faster convergence than steepest descent directions by searching along conjugate direction. The Quasi-Newton Technique is faster than the conjugate gradient technique, but it is complex and expensive to compute the Hessian matrix for feedforward NNs. These two algorithms lead to little acceptable result when the nonlinearity is heavy.

The Levenberg-Marquardt Technique (LMT) is an iterative technique that locates the minimum of a multivariate function expressed as the sum of squares of nonlinear real-valued functions. It has become a standard technique for nonlinear least-squares problems [27], widely adopted in a broad spectrum of disciplines. The LMT can be thought of as a combination of Backpropagation Algorithm and the Quasi-Newton Technique [34]. When the current solution is far from the correct one, the algorithm behaves like a Backpropagation Algorithm: slow, but guaranteed to converge. When the current solution is close to the correct solution, it becomes a Quasi-Newton method.

With the LMA, the increment of the trainable parameters vector can be calculated as follows:

$$\Delta\psi = [J^T J + \lambda I]^{-1} J^T e \tag{10}$$

where ψ is the trainable parameters vector; I is identity matrix; J is the Jacobian matrix and λ is the learning rate which automatically adjust during learning phase;

e is the cumulative error vector, it can be written as follows:

$$e = \left[e_{11}\ e_{21}\ \dots\ e_{s_2 1}\ e_{12}\ e_{22}\ \dots\ e_{s_2 2}\ \dots\ e_{1P}\ e_{2P}\ \dots\ e_{s_2 P}\right]^T$$

where P is number of input data, s_2 number of outputs.

$$e_{ji} = q_i(2,j) - T_i(j)$$

where $i = 1,2,\dots,P$ and $j = 1,2,\dots,S_2$.

If performance measure (MSE) in epoch $p+1$ is greater than the performance measure in epoch p, λ is divided by constant number ζ $(0 < \zeta < 1)$, whenever performance measure

decreased, λ is multiplied by ζ. Equation (5.25) shows that if λ is equal to zero the LMT becomes Quasi-Newton Technique (in this technique the increment of the trainable parameters vector $\Delta\psi = [J^T J]^{-1} J^T e$) and if μ is high the LMT becomes Backpropagation Algorithm.

The Jacobian matrix (it has $\beta \times s_2 P$ dimension) can be compute as follows:

$$[J] = \begin{bmatrix} \frac{\partial e_{11}}{\partial \psi_1} & \frac{\partial e_{11}}{\partial \psi_2} & \cdots & \frac{\partial e_{11}}{\partial \psi_\beta} \\ \frac{\partial e_{21}}{\partial \psi_1} & \frac{\partial e_{21}}{\partial \psi_2} & \cdots & \frac{\partial e_{21}}{\partial \psi_\beta} \\ \vdots & \vdots & \cdots & \vdots \\ \frac{\partial e_{m1}}{\partial \psi_1} & \frac{\partial e_{m1}}{\partial \psi_2} & \cdots & \frac{\partial e_{m1}}{\partial \psi_\beta} \\ \vdots & \vdots & \cdots & \vdots \\ \frac{\partial e_{1P}}{\partial \psi_1} & \frac{\partial e_{1P}}{\partial \psi_2} & \cdots & \frac{\partial e_{1P}}{\partial \psi_\beta} \\ \frac{\partial e_{2P}}{\partial \psi_1} & \frac{\partial e_{2P}}{\partial \psi_2} & \cdots & \frac{\partial e_{2P}}{\partial \psi_\beta} \\ \vdots & \vdots & \cdots & \vdots \\ \frac{\partial e_{s_2 P}}{\partial \psi_1} & \frac{\partial e_{s_2 P}}{\partial \psi_2} & \cdots & \frac{\partial e_{s_2 P}}{\partial \psi_\beta} \end{bmatrix}_{(\beta \times s_2 P)}$$

where β is the total number of trainable parameters in neural network which must be optimized; e_{kp} is the error of k^{th} output at p^{th} epoch.

Therefore, trainable parameters vector can be updated as follows:

$$\psi^{p+1} = \psi^p + \Delta\psi = \psi^p + [J^T J + \lambda I]^{-1} J^T e \qquad (11)$$

5. Design of the Neural Controller

Neural Networks (NNs) are capable of handling complex and nonlinear problems, process information rapidly and can reduce the engineering effort required in controller model development. Figure 3 depicts the controlled vehicle system with a neural controller as a key component. A neural controller has been designed to generate suitable control signals. The control signals will be applied as a control input signals to govern the hydraulic actuators to generate suitable damping forces for improving the vehicle performance. To find the optimal values of the trainable parameters of the neural controller for driving the plant to meet all control objectives, FOPID controllers should be designed (the details for the full design of FOPID controller for full vehicle nonlinear suspension systems are described in Reference [35]). In author's work, the input and output data obtained from the FOPID controller should

be used to train the parameters of neural controller using the LM Training Algorithm. Figure 4 depicts the training phase of the Neural Controller.

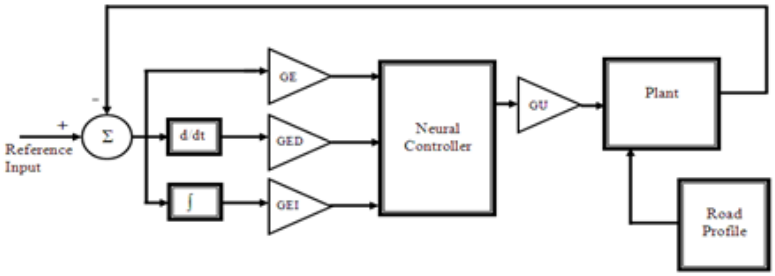

Figure 3 Neural Controller for a Full Vehicle Model

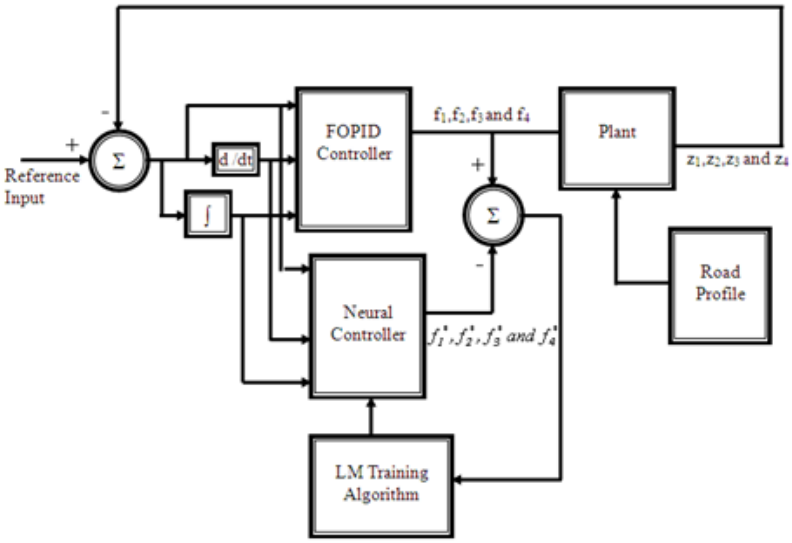

Figure 4 Training Phase of Neural Controller

After the optimal values of trainable parameters are obtained the neural controller design should be improved by adjusting the scaling gains, i.e. GE, GED, GEI and GU, as shown in Figure 3. To select the optimal values of the scaling gains, four-dimensional Golden Section Search (4-D GSS) method is introduced to reduce the trial time (For more detail about 4-D GSS method, see Reference [36]).

6. Simulation and Results:

The input road profile is selected as a white noise random signal. To design the neural controller, the optimal parameters of the FOPID controllers should be obtained first using the EA. In author's work, the input and output data obtained from the FOPID controllers have been used to design the neural controllers. The LM Training Algorithm has been used to modify the trainable parameters to track the output data obtained from the FOPID controllers. Four neural controllers have been designed, in which one for each suspension. To improve the

performance of the neural controller the scaling gains should be adjusted. The 4-D GSS method has been used to adjust the scaling gains (GE, GED, GEI and GU). As the result, the optimized values of scaling gains are 4, 3, 10 and 0.5, respectively.

All vehicle body variables, including vertical displacement at the centre of gravity: z_c, vertical displacement at P_3: z_3, pitch angle: α and roll angle: η, depend on the vertical displacements at points P_1, P_2 and P_4 (z_1, z_2 and z_4, respectively). The suspension deflection ($z_i - w_i$) and body acceleration ($\ddot{z}_c$) are used to evaluate the road handling and riding comfort of the passengers, respectively. By supplying the control signal, it is expected that just the vertical displacements of sprung mass (z_i) and body acceleration ($\ddot{z}_c$) will be targeted to reduce while the vertical displacements of unsprung masses (w_i) are not concerned. Therefore, when z_i decreases, the road handling performance will be improved while body acceleration decreases, the riding comfort is improved. In this paper just the responses of the vertical displacements at P_1, P_2 and P_4 and the body acceleration have been shown for comparison. In Figures 5-7 the responses of vertical displacements at P_1, P_2 and P_4 are compared, respectively. Figure 8 shows the response of the acceleration at the vehicle's centre of gravity. From these figures it can be seen that the neural controller is powerful and efficient.

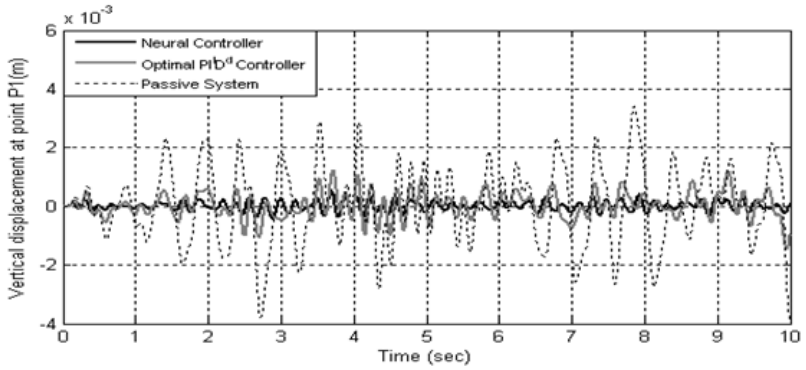

Figure 5 Time Response of Vertical Displacement at P_1

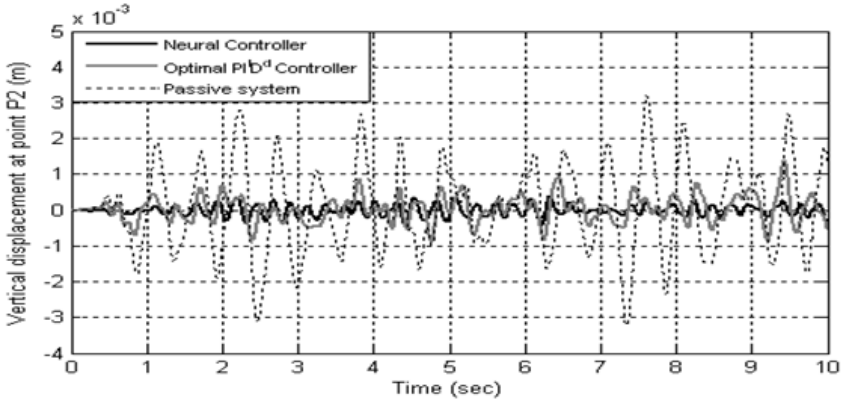

Figure 6 Time Response of Vertical Displacement at P2

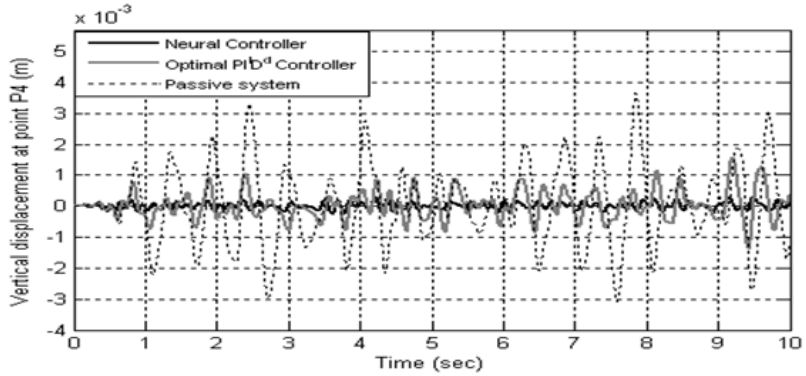

Figure 7 Time Response of Vertical Displacement at P4

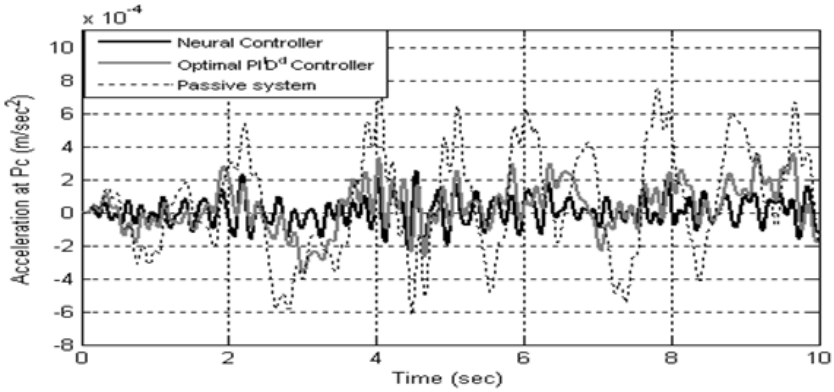

Figure 8 Time Response of Acceleration at Pc

The efficient controller is the controller that is still stable even the disturbance signals are applied on the plant. Therefore, to establish the effectiveness of any controller the robustness should be examined. After the optimal values of the trainable parameters of the neural controllers have been obtained, the robustness of the proposed neural controllers with optimal values should be tested. Six types of disturbances are applied in turn to test the robustness of the neural controller.

A. Square input signal with varying amplitude is applied as road input profile

The square input signal with fixed frequency (1 Hz) has been applied as road input profile. The amplitude of this signal has been changed from 0.01m to 0.08m. At each amplitude value, the cost function (as described in equation 12) has been calculated:

$$\phi = 0.5 \sum_{\varepsilon=1}^{4} z_{\varepsilon}^{2} \qquad (12)$$

Figure 9 shows the response of the cost function as function of amplitude of square signal input.

B. Sine wave input signal with varying amplitude is applied as road input profile

The different amplitude of sine wave input from 0.01m to 0.08m has been applied as road profile input (with fixed frequency (1 Hz)). The response of the cost function for the full vehicle without control, the result of optimal FOPID controller and neural controller are shown together in Figure10.

C. Square input signal with varying frequency is applied as road input profile

The square input with fixed amplitude (0.03 m) has been applied as road profile. The frequency of the input signal has been changed from 0.1Hz to 20Hz. The cost function has been calculated for each value of square input frequency. Figure 11 shows the cost function against different values of the square input frequencies.

D. ***Square input signal with varying frequency is applied as road input profile***

A sine wave input with different frequencies (from 0.1Hz to 20Hz) has been applied with fixed amplitude (0.03) to test the robustness of the proposed controller. Figure 12 shows the cost function against different values of the sine wave input frequencies.

E. Bending inertia Torque (T_x) is applied as road input profile

The value of bending torque (from 1000 Nm to 9000Nm) in addition to random signal as road profile has been applied. The cost function response is plotted as function of bending torque (T_x) in Figure 13.

F. Breaking inertia Torque (T_y) is applied as road input profile

The value of breaking torque (from 1000 Nm to 9000Nm) in addition to random signal as road profile has been applied. In Figure 14, the cost function response is plotted as function of braking torque (T_y).

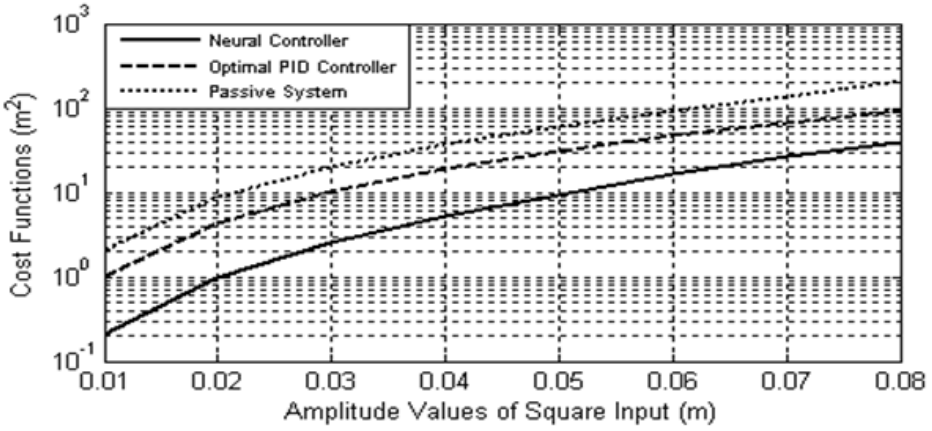

Figure 9. Response of the Cost Functions Against the Different Amplitude of Square Input.

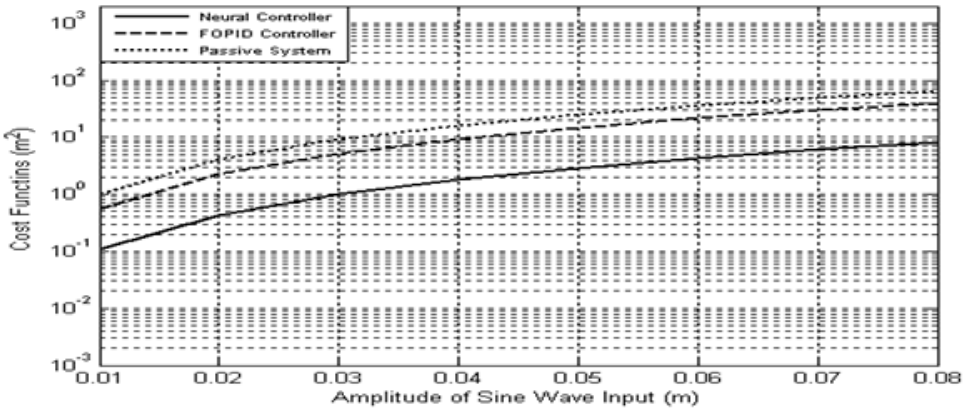

Figure 10 Response of the Cost Functions Against the Different Amplitude of Sine Wave Input.

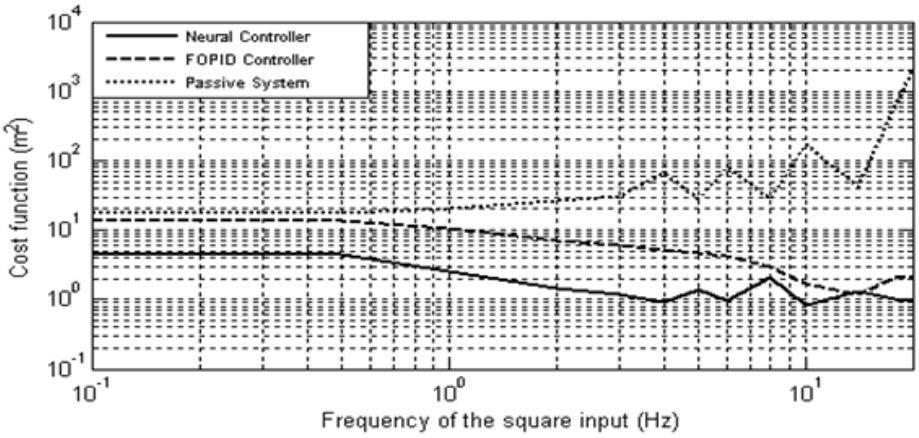

Figure 11 Response of the Cost Function Against Different Values of Square Input Frequencies

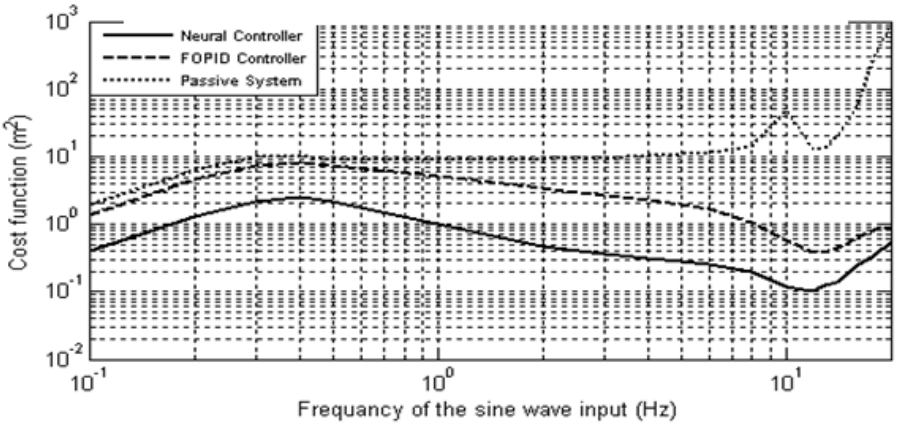

Figure 12 Response of the Cost Function Against Different Values of Sine Input Frequencies

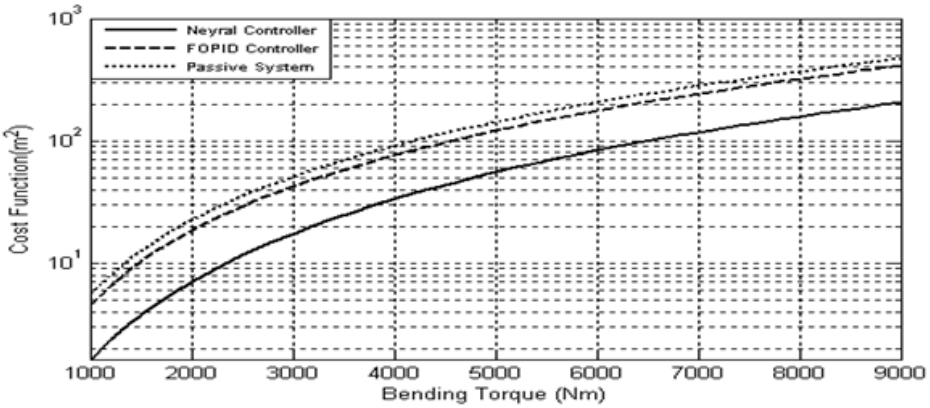

Figure 13 Response of the Cost Functions Against Bending Torque (Tx)

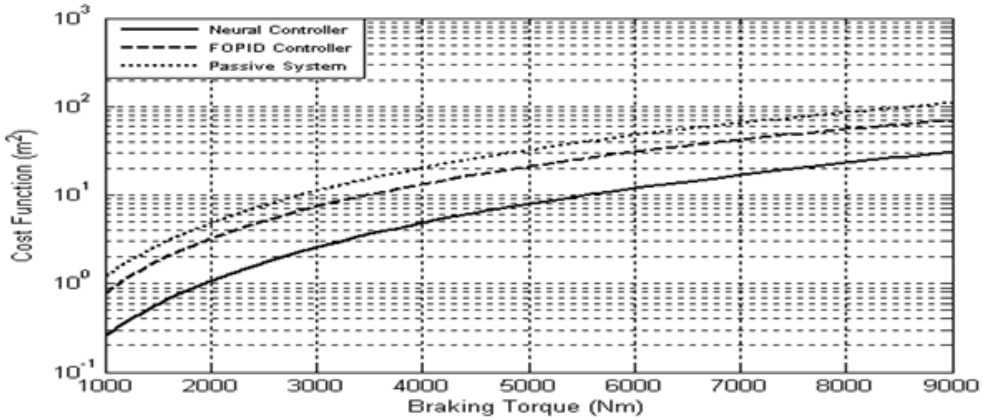

Figure 14 Response of the Cost Functions Against Braking Torque (Ty)

It is clear that in the above six cases, the cost functions of the neural controller are all below the corresponding FOPID controller and passive system.

7. Conclusion

The simulation results of the proposed neural controller indicate that the proposed controller enables the vertical displacement at each body suspension point to become much smaller than the responses of the corresponding FOPID controller and passive system. It has been confirmed that the proposed controller is more robust than the FOPID controller. Six different road profiles acting as the system input have been applied to assess the robustness of the proposed controller under disturbances. The test of the robustness proves that the neural controller is still stable and it forces the cost function to be minimum even significant disturbances occurred.

The proposed controller just has one neural network, which means it will be more economic than the other neural network controllers, such as model reference adaptive neural control, model predictive neural control, nonlinear internal model neural control, adaptive

inverse neural control system or neural adaptive feedback linearization. In all of these methods a minimum of two neural networks to design the controller are used (in the adaptive inverse control system it must be used three neural networks to design the controller) one as identifier and other one as controller.

References

[1] Sung, K., et al., *Discrete-time Fuzzy Sliding Mode Controller for a Vehicle Suspension System Featuring an Electrorheological Fluid Damper.* Smart Materials and Structures, 2007. **16**: pp. 798-808.

[2] Kuo, Y. and T. Li, *GA_Based Fuzzy PI/PD Controller for Automotive Active Suspension System.* IEEE Transactions on Industrial Electronics, 1999. **46**(6): pp. 1051-1056.

[3] Feng, J. and F. Yu, *GA-Based PID and Fuzzy Logic Controller for Active Vehicle Suspension System.* International Journal of Automotive Technology, 2003. **4**(4): pp. 181-191.

[4] Smith, M. and G. Walker, *Performance Limitations and Constraints for Active and Passive Suspensions: a Mechanical Multi-port Approach.* Vehicle System Dynamics, 2000. **33**(3): pp. 137-168.

[5] Biglarbegian, M., W. Melek, and F. Golnaraghi, *A Novel Neuro-fuzzy Controller to Enhance the Performance of Vehicle Semi-active Suspension Systems.* Vehicle System Dynamics, 2008. **46**(8): pp. 691-711.

[6] Yue, L., C. Tang, and H. Li, *Research on Vehicle Suspension System Based on Fuzzy Logic Control*, in *International Conference on Automation and Logistics*. 2008: Qingdao, China.

[7] Biglarbegian, M., W. Melek, and F. Golnaraghi, *Design of a Novel Fuzzy Controller to Enhance Stability of Vehicles*, N.A.F.I.P. Society, Editor. 2007. pp. 410-414.

[8] Kumar, M., *Genetic Algorithm-Based Proportional Derivative Controller for the Development of Active Suspension System.* Information Technology and Contro, 2007. **36**(1): p. 58-67.

[9] He, Y. and J. Mcphee, *A design methodology for mechatronics vehicles: application of Multidisciplinary optimization, multibody dynamics and genetic algorithms.* Vehicle System Dynamics, 2005. **43**(10): pp. 697-733.

[10] Gaspar, P., I. Szaszi, and J. Bokor, *Design of Robust controller for Active vehicle Suspension Using the Mixed μ Synthesis.* Vehicle System Dynamics, 2003. **40**(4): pp. 193-228.

[11] Chamseddine, A., H. Noura, and T. Raharijana, *Control of linear Full Vehicle Active Suspension System Using Sliding Mode Techniques*, in *International Conference on Control Applications*. 2006: Munich, Germany.

[12] March, C. and T. Sjim, *Integrated Control of Suspension and front Steering to enhance Vehicle Handling.* Processing IMechE, 2006. **221 Part D**: pp. 377-391.

[13] Li, S., S. Yang, and W. Guo, *Investigation on Chaotic Motion in Hysteretic Non-linear Suspension System with Multi-frequency Excitations.* Mechanics Research Communication 2004. **31**: pp. 229-236.

[14] Dixon, J., *The Shock Absorber Handbook*. 1999, USA: Society of Automotive Engineers, Inc.

[15] Joo, D., et al., *Nonlinear Modelling of Vehicle Suspension System*, in *Proceeding of the American Control Conference*. 2000: Chicago, Illinois.

[16] Hussain, M., *Review of the applications of neural networks in chemical process control. Simulation and on-line implementations.* Artificial Intelligence engineering 1999. **13**: pp. 55-68.

[17] Norgaard, M., O. Ravn, and N. Poulsen, *NNSYSID and NNCTRL tools for system identification and control with neural networks.* Computing and Control Engineering Journal 2001. **23**: pp. 29-36.

[18] Lera, G. and M. Pinzolas, *Neighborhood Based Levenberg-Marquardt Algorithm for Neural Network Training.* IEEE Transactions on Neural Networks 2002. **13**(5): pp. 1200-1203.

[19] Martin, T. and B. Mohammed, *Training Feedforward Networks with Marquardt Algorithm.* IEEE Transaction on Neural Networks, 1994. **5**(6): pp. 989-993.

[20] Ando, Y. and M. Suzuki, *Control of Active Suspension Systems Using the Singular Perturbation method.* Control Engineering Practice, 1996. **4**(33): pp. 287-293.

[21] Merritt, H., *Hydraulic Control Systems*. 1969, USA: John Wiley and Sons,Inc.

[22] Rumelhart, D., G. Hinton, and R. Willams, *Learning representations by back-propagation error*. Nature, 1986: pp. 533-536.

[23] Narendra, K. and K. Parthasarathy, *Identification and Control of Dynamical Systems Using Neural Network* IEEE Transaction on Neural Network, 1990. **1**(1): pp. 4-27.

[24] Sharkaway, A., *Fuzzy Control for the Automobiles Active Suspension System.* Vehicle System Dynamics, 2005. **43**(11): pp. 795-806.

[25] Samarasinghe, S., *Neural Network for Applied Sciences and Engineering.* Taylar and Francis Group LLC, 2007.

[26] Yue, L., C. Tang, and H. Li, *Research on Vehicle Suspension System Based on Fuzzy Logic Control*, in *International Conference on Automation and Logistics*. 2008: Qingdao, China. p. 1817-1821.

[27] Wilamowski, B.M., et al., *An Algorithm for Fast Convergence in Training Neural Networks*, in *International Joint Conference on Neural Networks*. 2001: Washington, DC pp. 1778-1782.

[28] Vogl, T.P., et al., *Accelerating the convergence of the backpropagation method.* Biological Cybernetics, 1988. **59**: pp. 257-263.

[29] Tollenaere, T., *Super SAB: Fast adaptive back propagation with good scaling properties.* Neural Network, 1990. **3**: pp. 561-573.

[30] Rigler, A.K., J.M. Irvine, and T.P. Vogl, *Rescaling of variables in back propagation learning.* Neural Network, 1991. **4**: pp. 225-229.

[31] Peng, C. and D. Magoulas, *Adaptive Non monotone Conjugate Gradient Training Algorithm For Recurrent Neural Networks*, in *19th IEEE International Conference on Tool with Artificial Intelligence.* 2007. pp. 374-381.

[32] Ishikamn, T., Y. Tsukui, and M. Matsunami, *Optimization of Electromagnetic Device Using Artificial Neural Network with Quasi Newton Algorithm.* IEEE Transaction on Magnetics, 1996. **32**(3): pp. 1226-1229.

[33] Lera, G. and M. Pinzolas, *Neighborhood Based Levenberg Marquardt Algorithm for Neural Network Training.* IEEE Transaction on neural Networks, 2002. **13**(5): pp. 1200-1203.

[34] Suratgar, A.A., M.B. Tavakoli, and A. Hoseinabadi. *Modified Levenberg Marquardt Method for Neural Networks Training*. in *Proceedings of World Academy of Science, Engineering and Technology*. 2005.

[35] Aldair, A. and W. Wang, *Design of Fractional order Controller Based on Evolutionary Algorithm for a Full Vehicle Nonlinear Active Suspension System.* International journal of Control and Automation (IJCA), 2010. **3**(4): pp. 33-46.

[36] Chang, Y., *N-Dimension Golden Section Search: Its Variants and Limitations.* 2nd International conference on Biomedical Engineering and Informatics, BMEI'09, 2009: pp. 1-6.

Authors

Ammar Aldair was born in Basrah, Iraq. He received his B.Sc. Degree in Electrical Engineering from University of Basrah, Iraq in 2000. In 2003, he received his M.Sc. Degree in Control and Systems Engineering from University of Basrah, Iraq. From 2003-2008, he was a Lecturer in the Electrical Department, University of Basrah, Iraq. He taught many subjects such as: Mathematics, Logic Systems, Electrical Circuits, Electronic Circuits, Control Systems and Advance Control Systems. In 2008, he had a scholarship from the Iraqi government to get the DPhil Degree in Intelligent Control Systems from the UK. Currently, he is a DPhil student in the School of Engineering and Design, University of Sussex, UK. His current research interests are in Intelligent Control Systems.

Weiji Wang was born in China. He received his DPhil degree from Oxford University in 1993. Currently he is a senior lecturer in the School of Engineering and Design, University of Sussex. His current research interests include Automotive Dynamics and Control.